8

Current Optical Imaging Techniques for Brain Tumor Research: Application of *in vivo* Laser Scanning Microscopy Imaging with a Cranial Window System

Kyuha Chong[1], Taeyun Ku[1], Kyungsun Choi[1],
Myunghwan Choi[2], Jonghee Yoon[1] and Chulhee Choi[1]
[1]*Korea Advanced Institute of Science and Technology (KAIST),Yuseong-gu, Daejeon,*
[2]*Wellman Center for Photomedicine,*
Massachusetts General HospitalCambridge, Massachusetts,
[1]*Republic of Korea*
[2]*United States of America*

1. Introduction

"Seeing is believing." This may not be true in all areas of biomedical research, but identifying cellular characteristics of tumors and specifying their anatomical locations are the most important processes for diagnosing and treating tumors. Furthermore, various imaging techniques with various modalities have been introduced to investigate disease progression, track the pharmacokinetic behavior of drugs, and in clinical applications.

Reconstructing images at the molecular level has been realized with the dramatic advancement in energy sources, detectors, computational methods, and instruments. Computed tomography (CT), magnetic resonance imaging (MRI), positron emission tomography (PET), and ultrasound imaging are well-known imaging techniques that have tremendously improved not only preclinical research but also clinical treatment. Contrast-enhanced CT, MRI and PET have permitted non-invasive detection of abnormal tissues, particularly for tumor research and clinical applications.

Imaging techniques currently used for brain tumor research vary with purpose and imaging characteristics. The techniques can be grouped by three aspects: (1) energy, (2) spatial resolution, and (3) type of information obtained (Weissleder & Pittet, 2008). The energies generally used for these techniques are X-rays (e.g., classic X-ray imaging, CT, multi-detector CT), magnetic fields (e.g., MRI and diffusion MRI), positrons (e.g., PET), sound waves (e.g., ultrasound imaging, interventional ultrasound imaging), photons (e.g., bioluminescence imaging, fluorescence reflectance imaging, fluorescence-mediated tomography, and laser scanning microscopy imaging), and combinations of such modalities (e.g., PET-CT, PET-MRI, CT, or MRI with fluorescence-mediated tomography). The techniques can also be distinguished by spatial resolution and the information obtained: (1) macroscopic, (2) mesoscopic, and (3) microscopic or (1) anatomical, (2) physiological, and (3) cellular and molecular.

Optical imaging techniques (OITs) are a subset of imaging modalities that mainly use photons as their energy source. The beauty of these techniques is that the cellular or molecular level of the target can be visualized and target location or texture can be identified with different dyes (Kovar et al., 2007; Massoud & Gambhir, 2003). Although OITs have limited imaging depth and procedure accessibility, they have become indispensable in many fields of research and clinical applications, including brain tumor research.

2. OITs for brain tumor research

Tremendous technological improvements and an increase in the number of OIT applications have occurred with advances in optics and probes. Visualization of the structures and functions of the brain has become possible with microscopic and macroscopic imaging techniques. Because of these advances, OITs have been actively utilized in the field of brain research.

Ultraviolet, visible, and infrared light are the main spectrums of the light used in OITs. The energy (E) of photons is denoted by wavelength (λ). Photons with a shorter wavelength have higher energy than those with a longer wavelength, which is given by the following equation:

$$E = \frac{hc}{\lambda}$$

where h is Planck's constant and c is the speed of light.

Spectrum Spatial resolution	Visible light (380-780nm)	Near-infrared (650-1400nm)
Macroscopic	Bioluminescence imaging (BLI)	Near-infrared fluorescence (NIRF) imaging
Microscopic	Confocal laser scanning microscopy (CLSM) imaging	Multi-photon laser scanning microscopy (MPLSM) imaging

Table 1. Frequently used optical imaging techniques for *in vivo* studies

Although tissue penetration by photons varies with the type of tissue, longer wavelength light generally penetrates deeper; less than 1 mm at 400 nm (blue), 0.5 to 2 mm at 514 nm (green), 1 to 6 mm at 630 nm (red), and 1 to 2 cm at 800 nm (near-infrared) (Barolet, 2008; Kalka et al., 2000; Wilson & Patterson, 1986). Penetration depth for a human brain tumor was reported to be 1 mm at 514 nm, 2.5 mm at 635 nm, and 6 mm at 1060 nm (Svaasand & Ellingsen, 1985).

Spatial resolution and the biological level of information should also be considered for imaging. The primary macroscopic imaging information is physiological, cellular, and molecular, and screening of molecular events or cell tracking is possible with OITs. Higher resolution images to obtain anatomical and quantitative information can be attained with microscopic imaging. But both macroscopic and microscopic imaging have depth and coverage limitations, which are regulated by the chosen wavelength and fluorophore (Wiesner et al., 2009).

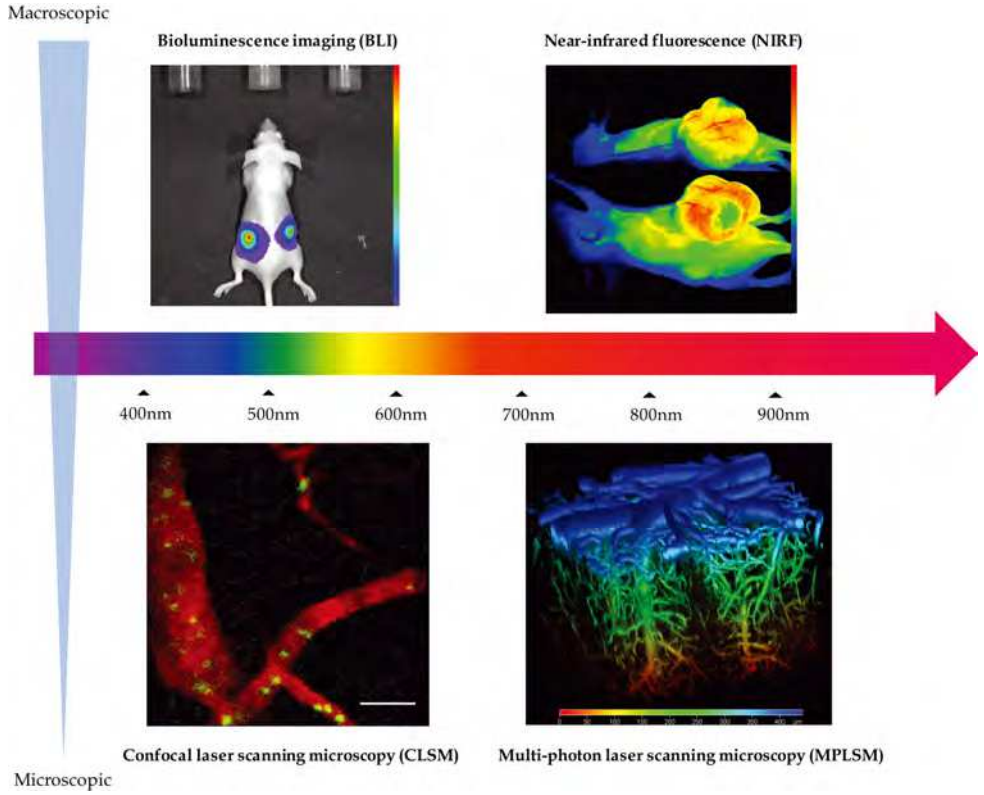

Fig. 1. Schematization of the most frequently used optical imaging techniques for *in vivo* studies. The bar in the middle indicates the light spectrum.

The most frequently used OITs for *in vivo* brain tumor studies are bioluminescence imaging (BLI), near-infrared fluorescence (NIRF) imaging, confocal laser scanning microscopy (CLSM) imaging, and multi-photon laser scanning microscopy (MPLSM) imaging (Table 1 and Fig. 1). These OITs are categorized by light spectrum and spatial resolution. Using a particular technique is determined by the needs and purposes of the research and by considering the technique characteristics (Table 2).

2.1 BLI

BLI is a non-invasive macroscopic imaging technique that uses luminescence for imaging. The chemical reaction between luciferase and luciferin (d-(-)-2-(60-hydroxy-20-benzothiazolyl)-thiazone-4-carboxylic acid) in the presence of oxygen and adenosine triphosphate transforms chemical energy into luminescence at a wavelength of 560 nm. Cells engineered to express luciferase emit light in the presence of luciferin (Ozawa & James, 2010; Sun et al., 2010).

A luciferin substrate is administered via an intraperitoneal injection, and images obtained 10 to 20 minutes after injection for tumor imaging in luciferase-expressing tumor xenograft models. The beauty of this technique is not only that it is non-invasive and rapid but that it

is highly sensitive, because there is no inherent light background noise (Wiesner et al., 2009). Tumor development, growth, and location can be quantitatively and noninvasively analyzed with BLI (Rehemtulla et al., 2000).

Although BLI has many benefits, there are several drawbacks. The transmission efficiency of bioluminescence largely depends on the type of tissue and the depth of origin, due to the scattering properties of visible light. Disturbances in the light transmission due to light absorption by hemoglobin and signal attenuation by melanin and fur also limit application of BLI (O'Neill et al., 2010). Additionally, even though advances have been made to translate BLI data into three-dimensional (3D) tomographic imaging (Chaudhari et al., 2005; Slavine et al., 2006), commonly used BLI has limited use for 3D reconstruction.

Technique	Resolution	Depth	Time	Imaging agent	References
BLI	Several mm	cm	Minutes	Luciferin	(O'Neill et al., 2010; Rehemtulla et al., 2000; Sun et al., 2010)
NIRF	Several hundred µm	cm	Minutes	Near-infrared fluorophore	(Choi et al., 2011; Kircher et al., 2003; Veiseh et al., 2007)
CLSM	0.5-1.0 µm	< 100-200 µm	Second to hours	Fluorophore, photoprotein	(Centonze & White, 1998; Gratton, 2011)
MPLSM	0.5-1.0 µm	< 500-1,000 µm	Second to hours	Fluorophore, photoprotein	(Calabrese et al., 2007; Farrar et al., 2010; Levene et al., 2004; Theer et al., 2003; Winkler et al., 2009; Winkler et al., 2004)

Table 2. Overview of optical imaging techniques for *in vivo* studies

2.2 NIRF imaging

NIRF imaging is an efficient, non-invasive, and high-throughput modality useful for *in vivo* imaging (Hsu et al., 2006). NIRF imaging uses near-infrared fluorophores, whether the reflectance technique is applied or not. Because NIRF (650–900 nm) penetrates deeper into tissue than luminescence (Shah & Weissleder, 2005) and does not require cellular transfection, NIRF imaging is regarded as a more effective technique for brain tumor studies than that of BLI.

However, because data acquisition is based on a two-dimensional planar image, NIRF imaging is limited for 3D reconstruction. Additionally, NIRF imaging has problems of light scattering and low quantum efficiency, due to longer wavelengths, which leads to lower signal intensity (Amiot et al., 2008). Although NIRF penetrates deeper than BLI (up to several centimeters), the depth is not adequate to analyze deeper targets within a large animal. Thus, at present, this imaging modality, which uses traditional NIRF fluorophores, is suitable only for small animals such as rodents.

Currently used NIRF materials are fluorescent dyes, quantum dots, single-walled carbon nanotubes, and rare earth metal reagents (Amiot et al., 2008). Because such fluorophores do not have specific targets, molecular modifications are required to specify targets. Specificity is achieved by combining targeting molecules with fluorophores such as Cy5.5-chlorotoxin

(Veiseh et al., 2007). Vascular leakiness can be utilized for brain tumor imaging. Indocyanine green (ICG), an NIR fluorophore, has been used to analyze blood perfusion and permeability of tumors (Choi et al., 2011). Most ICG is bound to albumin in serum, so it does not normally leak into the extravascular space, but it does pass into highly leaky tumor vasculature. Rapid vascular normalization with neutralizing vascular endothelial growth factor was identified with this novel dynamic fluorescence imaging technique using ICG.

2.3 Laser scanning microscopy (LSM) imaging

Since CLSM was introduced in the late 1980s (Brakenhoff et al., 1985; Centonze & White, 1998), the acquisition of high resolution sectional imaging data has become practical, even with thick samples. CLSM collects information from selected foci using a pin-hole, which eliminates out-of-focus information. Phototoxicity in the area that is not the region of interest (ROI) and short penetration depth are major limitations of this technology.

MPLSM is a revolutionized fluorescence microscopy modality that uses non-linear optical properties such as multi-photon absorption. Near-infrared light, which is delivered with a high-power femtosecond pulse, excites fluorophores or molecules in a small specific spot with longer wavelength light (Gratton, 2011). MPLSM has been applied to intra-vital studies since the discovery of molecular excitation by simultaneous absorption of two photons (Denk et al., 1990).

Because MPLSM utilizes longer wavelength photons, image information can be acquired with minimal phototoxicity to the samples and with deeper penetration compared with conventional CLSM. Up to 800–1,000 μm depth resolution is achievable with an MPLSM system (Theer et al., 2003; Weissleder & Pittet, 2008), but typically < 500 μm depth of resolution is achievable for brain imaging (Levene et al., 2004).

However, it remains technically challenging, as significant decreases in resolution occur at greater depths. So, these techniques are inappropriate for deep tissue (> 1 cm depth) imaging. Furthermore, samples or specimens must be prepared with more invasive methods for *in vivo* brain tumor imaging, such as the dorsal skin-flap chamber or cranial window methods, as compared with BLI or NIRF imaging. Although lower energy photons are transmitted into the sample than with BLI or NIRF, fluorophore photo-bleaching frequently occurs, particularly with repetition.

3. Animal models for brain tumor research

In vivo animal model studies are very important for translating biological assessments. Many methods and techniques are available to create animal models that mimic the pathology and tumor environment of a human brain tumor. The tumor model type is chosen depending on the experimental conditions and study purposes.

The xenograft tumor model (XM) is one of the most common and powerful methods to mimic tumor status. XM has been widely used for interventional studies due to convenience. However, the genetically engineered mouse model (GEMM) is preferred for results because of the difference between cell origin and an inability to represent the mechanism of tumor development. However, difficulty producing the model, late onset, insufficient representation of the evolving microenvironment with additional stochastic genetic events, and the inherent difficulty of tumor diagnosis in a timely fashion makes GEMM less desirable (de Vries et al., 2010; Huse & Holland, 2009). Table 3 is an overview of the animal models currently used for brain tumor studies.

Type	Subtype	Realization	Lead time	Relevance	Imaging technique used	References
Genetically engineered mouse model (GEMM)	Germline modification	Highly difficult	Several months to years	High	BLI, NIRF	(Fomchenko & Holland, 2006; Huse & Holland, 2009)
	Somatic cell gene transfer	Difficult	Weeks to months	Intermedate to high	BLI, NIRF	(de Vries et al., 2010; Wiesner et al., 2009)
Xenograft tumor model (XM)	Subcutaneous transplant	Easy	Weeks to months	Low	BLI, NIRF	(Choi et al., 2011; O'Neill et al., 2010)
	Dorsal skin flap chamber	Intermediate	Several weeks	Low	LSM	(Hoffman, 2002; Tozer et al., 2005)
	Orthotopic, non-cranial window	Intermediate	Several weeks	Intermediate	BLI, NIRF	(Hashizume et al., 2010; Ozawa & James, 2010; Szentirmai et al., 2008)
	Orthotopic-cranial window	Difficult	Several weeks	Intermediate	LSM	(Calabrese et al., 2007; Farrar et al., 2010; Winkler et al., 2009; Winkler et al., 2004)

Table 3. Overview of animal models for brain tumor research ("imaging technique used" are those mainly used for *in vivo* imaging)

3.1 GEMM

GEMM is a tumor model generated by a particular genetic alteration. GEMM strongly recapitulates the tumorigenesis process and the nature of tumor progression. Thus, scientists appreciate the results that are obtained from this model. However, many GEMM express unexpected alterations in genes of other organs or tissues. In those cases, it is difficult to say whether GEMM fully presents tumorigenesis, so it is referred to as human cancer predisposition syndromes (Fomchenko & Holland, 2006). Because modifying a particular gene and achieving the target phenotype are very difficult to realize, this model is the first choice for an initial study.

GEMM includes transgene, knock-out, and knock-in mouse models. A transgenic mouse model contains additional genes for a certain purpose (Hanahan et al., 2007). A knock-out mouse model has one or more specific genes inactivated mainly by replacing or disrupting the coding exons, whereas a knock-in mouse model is one in which an endogenous sequence is exchanged with a mutated DNA sequence without disrupting any other genes (Manis, 2007).

There are many types of GEMMs that refer to brain tumors. These models mainly focus on gliomas and medulloblastomas, which are the most common brain tumors in humans. The main considerations for producing such models are as follows: genetics, tumorigenesis mechanism of the model (conventional and/or conditional, transgenic and/or knock-out), incidence of successful tumor development, histological or morphological grades (Huse & Holland, 2009), development type (*de novo* or progressive) (Kwon et al., 2008), the possibility of recapitulation, and organ or area specificity (Huse & Holland, 2010).
Advances have been made in production methods to overcome the inconveniences and uncertainties of traditional GEMM, which are derived from germline modification strategies. Somatic cell gene transfer is a method that generates a genetically altered tumor using viral or pegylated DNA plasmids. While traditional GEMM is used to spontaneously develop a tumor in any location, the somatic cell gene transfer model forces the alteration to a specific location, which is very important for imaging.
For example, de Vries et al. developed a high-grade glioma model using a stereotactic intracranial injection of lentiviral GFAP-Cre or CMV-Cre vectors into compound LoxP-conditional mice, p53;Ink4a/Arf;K-Ras^{v12} (de Vries et al., 2010). The mice developed a tumor within 25 days after injection. They obtained information about the existence of the tumor at an early stage using BLI. They also provided evidence for therapeutic interventional studies by comparing the alterations and differences in tumor growth between a control and a chemotherapy treatment group using longitudinal BLI analysis.
Although somatic cell gene transfer models can predict tumor location, the tumor usually originates in a deep brain structure. Therefore, the OITs are limited to BLI or NIRF imaging. It is affordable to use LSM imaging for GEMM; however, LSM imaging is mostly limited to sample slice imaging and is insufficient for *in vivo* studies.

3.2 XM

As mentioned previously, XM is the most frequently used model for *in vivo* tumor studies. The XM is created by implanting an established cell line or primary tumor cells into a particular location in the animal. The strengths and weaknesses of this technique are listed in Table 4 (Finkelstein et al., 1994; Fomchenko & Holland, 2006).

Strengths	Weaknesses
• Synchrony and reproducibility of tumor formation • Rapid tumor development • High penetrance • Easy tumor visualization	• Lack of stepwise genetic alteration • Alteration of the cells or cell line • Lack of histological accurate vascularization • Rare recapitulation of tumor-of-origin phenotype

Table 4. Strengths and weaknesses of the xenograft tumor model

The frequently used types of XM models for brain tumor studies can be summarized as follows: (1) subcutaneous transplant model, (2) dorsal skin-flap chamber model, (3) orthotopic, non-cranial window model, and (4) orthotopic-cranial window model. OITs can be used with these models, because of convenience and ability to specify the ROI.

3.2.1 Subcutaneous transplant model

The subcutaneous transplant model is simply made by injecting a tumor cell suspension in the flank or leg area of the animal. Tumor growth progression differs depending on cell characteristics but usually it takes several weeks to months to reach an adequate volume for study (Morton & Houghton, 2007). Usually 3×10^6–1×10^7 cells are needed for a successful implantation.

Interventional studies were classically performed by estimating tumor volume using direct length and width measurements (Jensen et al., 2008) or histopathological analysis such as immunohistochemistry. However, these estimates only provide relative values and are inherently biased, whereas histopathology can only be performed by excising the tumor. Because BLI and NIRF imaging provide non-invasive and semi-quantitative measurements, OITs have become a useful modality for longitudinal *in vivo* studies using this model.

In addition to quantifying tumor mass, an OIT modality can be used to measure functional vascular parameters (Choi et al., 2011). Vascular heterogeneity, density, and permeability of an implanted tumor can be estimated with a quantitative analysis of emitted signal intensity.

3.2.2 Dorsal skin-flap chamber model

Longitudinal *in vivo* optical studies are possible with minimal intervention if localized surgical implantation of the tumor is supported by fixing a transparent slide glass coverslip, such as in the dorsal skin-flap chamber (DSFC) model. More detailed and precise information can be obtained with the use of the LSM technique. Because MPLSM imaging has minimal phototoxicity and deeper penetration than some other modalities, minimally invasive and repetitive images are achievable with high resolution.

Using the LSM technique, the DSFC tumor model not only provides information about the tumor itself but also of the interaction between the tumor and tumor-associated vessels. Parameters such as inter-capillary distance, vessel length, and branching ratios can be analyzed (Tozer et al., 2005). Furthermore, 3D data facilitates a precise evaluation of tumor angiogenesis.

Implantation of the tumor is possible by either locating a tumor fragment or spheroid just above the upper tissue layer (Torres Filho et al., 1995) or by injecting a suspension of tumor cells above the fascia. The total cell count of the initial implantation is not fixed, and location and method of implantation can be varied depending on the study group. Regardless of which protocol is used, images can be acquired several weeks after injection.

3.2.3 Orthotopic, non-cranial window model

The orthotopic xenograft model offers more advanced synchrony of the brain tumor microenvironment than that of the subcutaneous transplant or DSFC models. Generally, a tumor is implanted with an inoculating cell line suspension containing 1×10^5–5×10^5 cells by stereotactic injection. Injection location varies among research groups. For example, implantation by Ozawa and James was 2 mm lateral to the bregma, 1 mm anterior to the coronal suture, and at a 3 mm depth from the underside of the skull (Ozawa & James, 2010); Hashizume et al. utilized an implantation protocol of 3 mm from the midline, just behind the bregma for supratentorial, and 3 mm from the midline, 1.5 mm behind the lambdoid suture for infratentorial, with a 3 mm depth from the bottom of the skull (Hashizume et al., 2010); and Szentirmai et al. performed surgery at 2.5 mm lateral and 0.5 mm posterior to the bregma and at a parenchymal depth of 3.5 mm (Szentirmai et al., 2008).

Implantation in deeper locations provides sufficient space and abundant vascular support for tumor growth but precludes intravital microscopic imaging. Early detection and time-series quantitative estimation of tumor growth are possible using BLI and NIRF imaging techniques.

3.2.4 Orthotopic-cranial window model

The orthotopic-cranial window model combines the benefits of window modeling, which enables microscopic evaluation, with the synchrony of an orthotopic xenograft. Complexity of realization is a drawback of this technique compared with other previously described xenograft models, but it is not as much as with GEMM. Researchers can efficiently achieve a model within several weeks with practice.

The tumor can be implanted by fragment or with a cell suspension. However, implantation methods vary between research groups, as compared to the non-cranial window model. We consider that the differences are mainly due to variations in the cranial window surgery method.

For example, Winker et al. attained the model by implanting 0.2–0.3 mm size tumor fragments at a depth of 0.4 mm (Winkler et al., 2004), whereas Farrar et al. injected 3×10^6–2×10^7 suspended cells at a depth of 1.75 mm with a 55° angle (Farrar et al., 2010). We believe that injecting a cell suspension volume of 3–5 µl containing 1×10^5–5×10^5 cells (Winkler et al., 2009) or up to 1×10^6 cells (Calabrese et al., 2007) at a depth of 0.5–2.0 mm from the bottom of the skull is adequate.

Theoretically, all OITs are applicable with this model, if cells and materials are properly prepared; however, MPLSM imaging is the first choice.

3.3 Metastatic brain tumor models

The brain tumor models discussed above are models for recapitulating primary or secondary brain tumors originating within the brain. Although most studies of primary and secondary brain tumors are ongoing, metastatic brain tumor studies are also conducted, because metastatic brain tumors have the highest incidence among all brain tumors. The XM is clearly more relevant to the metastatic process; therefore, model production methods are metaphysically the same as XMs.

A metastatic model can be produced by an entrancing method, as reported by Kienast et al. They realized a metastatic brain tumor model by injecting tumor cells via the carotid artery and demonstrated metastasis formation with MPLSM imaging and a cranial window (Kienast et al., 2010). Such a study was an excellent demonstration of how MPLSM imaging can be combined with the cranial window model.

4. Application of chronic cranial window model system with CLSM and TPLSM imaging for brain tumor research

An Orthotopic xenograft of a brain tumor with a cranial window system has emerged as a potent technique for brain tumor research because it is less costly and requires less lead time to manufacture an XM than a primary tumor model, and the researcher can select the ROI to perform the analysis in a time-dependent manner.

Thinned skull and open craniotomy (craniectomy) models are two types of cranial window systems. The main considerations relating to the two systems are invasiveness (Xu et al., 2007), feasible imaging depth, and maintenance duration of the window. Drew et al.

reported that chronic observations are possible with the thinned skull cranial window model (Drew et al., 2010). However, the thinned skull model can only be applied for metastatic brain tumor model which is created by intracardiac injection of metastatic tumor cells, or for some GEM brain tumor model which produces a tumor at the superficial cortical area. An open craniotomy is more suitable for LSM imaging of an orthotopic xenograft, regardless of whether dura matter must be removed (Orringer et al., 2010)

Now, we will introduce our xenograft model method, which we named the orthotopic xenograft-chronic cranial window (OxCCW) model. This model is based on previous studies and reports (Calabrese et al., 2007; Farrar et al., 2010; Winkler et al., 2009; Winkler et al., 2004). The OxCCW model preserves dura mater for avoidance of additional brain injury, convenience and a high success rate. The resulting images are obtained with CLSM and MPLSM imaging techniques.

4.1 OxCCW model

Red fluorescence protein (RFP) and green fluorescence protein (GFP) expressing U251 (U251-RFP and U251-GFP) tumor cells (human malignant glioma cell-line) were grown *in vitro* in Dulbecco's modified Eagle's medium (DMEM) with 10% fetal bovine serum, 1% non-essential amino acids, and 1% penicillin-streptomycin at 37°C under 20% O2 and 5% CO2. After harvesting, the cells were resuspended in serum-free DMEM medium for implantation into immunodeficient mice. The mouse head was fixed in a stereotactic frame. After the skin incision, a craniotomy was performed at the temporo-parietal area with a high-speed drill. A modified micropipette was introduced into a small incision in the dura at the trajectory point for the injection. In total, 2 x 10^5 cells in a 5 µl volume were injected at a depth of 0.5 mm from the bottom of the skull. After injection, the craniotomy area was covered with a slide glass coverslip and fixed with bone cement (Fig. 2).

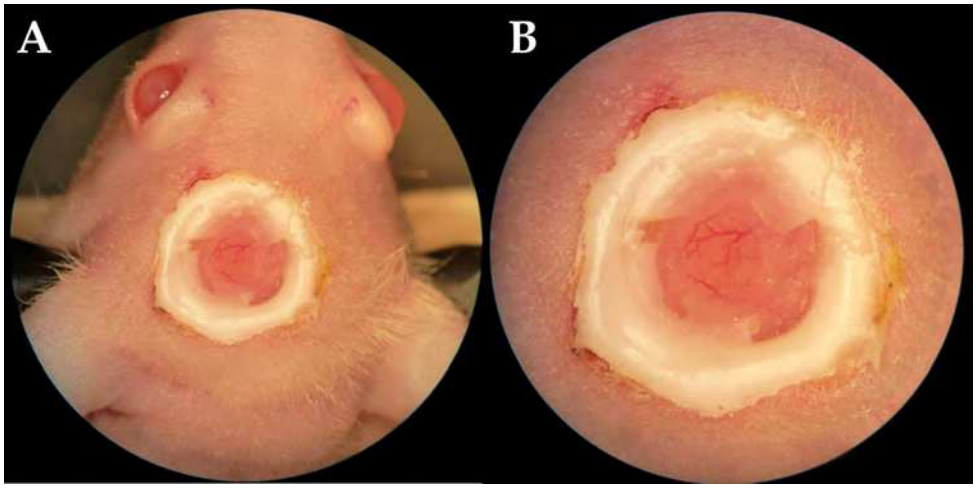

Fig. 2. Macroscopic inspection of orthotopic xenograft-chronic cranial window (OxCCW) model. A. 10X image. The cranial window was set at the left temporo-parietal area. B. 20X image. The slide glass coverslip was tightly fixed with bone cement. Pial vascular structures could be identified.

4.2 CLSM and MPLSM imaging of OxCCW

Time-series images using CLSM and MPLSM can be captured with the OxCCW model. CLSM images were obtained with 488 nm and 543 nm lasers, and MPLSM images were obtained with an 800 nm femtosecond pulsed laser. The growth and progression of the implanted tumor and vascular co-option processes were readily monitored. Vascular changes due to surgical injury (i.e., engorgement of superficial vessels), which were inevitable due to implantation, usually recovered within 1 week after the surgery (Fig. 3).

Acquisition of acceptable CLSM images was limited to a depth of 100 μm in our OxCCW model. Imaging of an area deeper than 100 μm was not impossible, but deeper depths revealed poorer resolution, and photo-induced injury occurred more frequently due to a need for more laser power. This problem with CLSM imaging can be solved with MPLSM imaging (Fig. 4). Theoretically, imaging to a depth of 500–1,000 μm is possible with MPLSM. In our experience, acceptable imaging depth of the OxCCW model was extended up to 300 μm from the pial surface using MPLSM imaging.

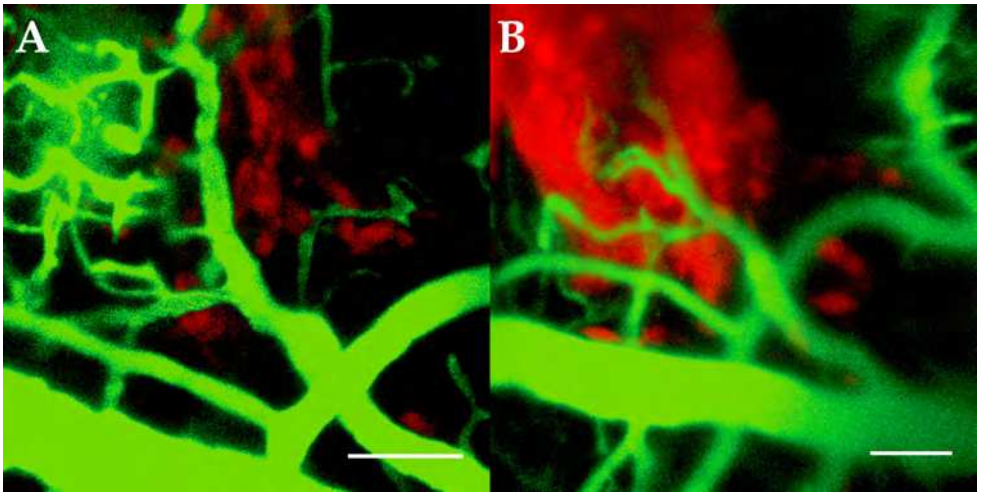

Fig. 3. Time-series confocal laser scanning microscopy images of the orthotopic xenograft-chronic cranial window (OxCCW) model. The images above are projections from the pial surface to a depth of 100 μm. In total, 2 x 10^5 U251-RFP cells were implanted 1 week before initial imaging. FITC-dextran (2 MDa) was intravenously injected for vascular imaging. (A, B) Tumor progression with the vascular co-option could be monitored with the imaging system. Red indicates emitted fluorescence from U251-RFP cells, and green indicates FITC-dextran. The interval between A and B was 1 week. Scale bar, 100 μm.

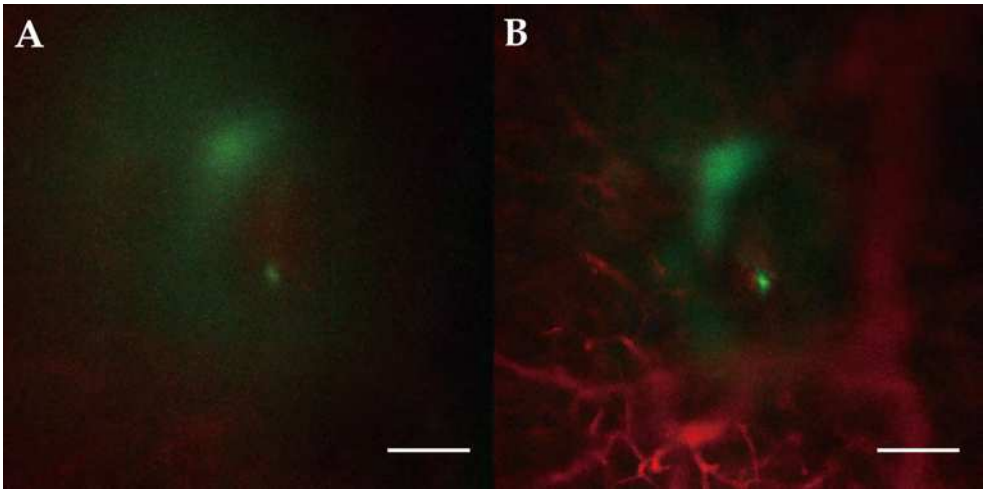

Fig. 4. Comparative confocal and multi-photon laser scanning microscopy images with the orthotopic xenograft-chronic cranial window model. In total, 2 x 10^5 U251-GFP cells were implanted 1 week before imaging. Rhodamin-dextran (70 kDa) was intravenously injected for vascular imaging. The imaging information was collected from a depth of 100–150 μm from the pial surface. Green indicates emitted fluorescence from U251-GFP cells and red indicates rhodamin-dextran. (A) Projection image from a confocal laser scanning microscope. (B) Projection image from a multi-photon laser scanning microscope. Scale bar, 100 μm.

5. Future perspectives

OIT applications are now beyond imaging itself and are not restricted by experimental boundaries. Intra-operative brain tumor imaging, to define the tumor area for resection, has already been applied in clinical settings. Fluorescence-guided surgical resection has been performed in an operating room using 5-aminolevulinic acid (5-ALA), a prodrug of fluorescent molecule protoporphyrin IX (PpIX), and useful statistical results were obtained (Stummer et al., 2006). In addition to the clinical application of OITs for diagnostic purposes, many attempts have been made to introduce therapeutic applications of OITs such as photodynamic therapy.

Combining optical technologies with OITs has been actively attempted for biomedical applications other than imaging. Our group recently reported utilizing a near-infrared femtosecond laser for minimally invasive molecular delivery into the brain (Choi et al. 2011). The delivery is acquired by optical modulation, which enhances the transient increase in vascular permeability (Fig. 5). Additionally, optical modulation of neurovascular coupling in combination with label-free optical activation of astrocytes was also demonstrated.

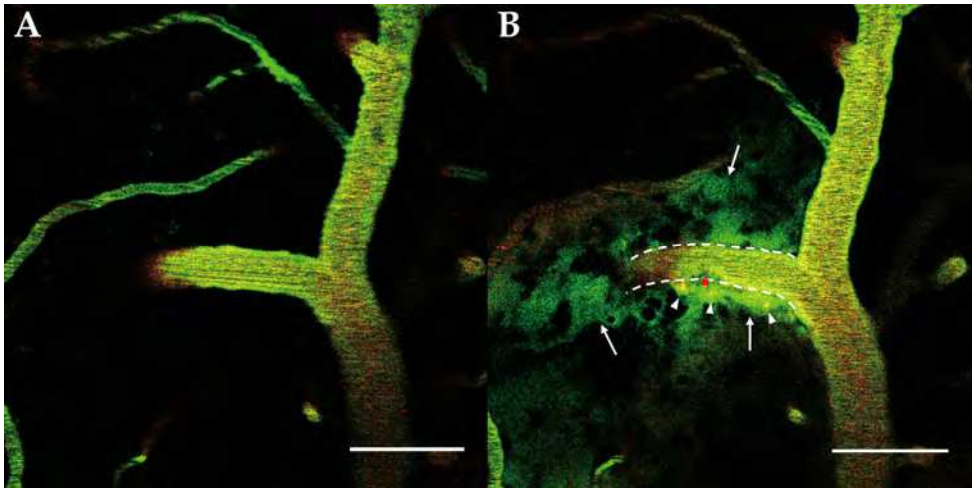

Fig. 5. Laser-induced vascular permeabilization. Imaging and optical modulation were performed with multi-photon laser scanning microscopy (800 nm, femtosecond pulsed laser). FITC-dextran (2 MDa) and fluorescent microspheres (FS03F/5147, Bangs Laboratories) were injected via the tail vein. Green and red indicate FITC-dextran and fluorescent microspheres, respectively. (A) Pre-permeabilization image. (B) Post-permeabilization image. Green dye (white arrows) and red fluorescent microspheres (white arrowheads) were extravasated after optical modulation. Red dot indicates the region that was optically modulated. White dotted line demarcates baseline lumen of the venule. Scale bar, 50 μm.

6. Conclusion

OITs have emerged as essential tools for intravital imaging. The most frequently used OITs are BLI, NIRF, and LSM imaging. Among them, MPLSM is the most potent imaging technique because it obtains precise intravital microscopic information. Translational and interventional studies are expected to be performed in a more efficient manner with the combination of MPLSM and the OxCCW system.

7. Acknowledgements

This research was supported by a grant (2009K001282) from the Brain Research Center of the 21st Century Frontier Research Program funded by the Ministry of Education, Science, and Technology, the Republic of Korea.
We are grateful to Prof. Gou Young Koh, Dr. Young Jun Koh and Junyeop Lee for their support of BLI imaging and their constructive discussions.

8. References

Amiot, C. L.; Xu, S. P.; Liang, S.; Pan, L. Y. & Zhao, J. X. J. (2008). Near-infrared fluorescent materials for sensing of biological targets. *Sensors,* Vol.8, No.5, pp. 3082-3105, ISSN 1424-8220

Barolet, D. (2008). Light-emitting diodes (LEDs) in dermatology. *Seminars in cutaneous medicine and surgery,* Vol.27, No.4, pp. 227-38, ISSN 1558-0768

Brakenhoff, G. J.; van der Voort, H. T.; van Spronsen, E. A.; Linnemans, W. A. & Nanninga, N. (1985). Three-dimensional chromatin distribution in neuroblastoma nuclei shown by confocal scanning laser microscopy. *Nature,* Vol.317, No.6039, pp. 748-9, ISSN 0028-0836

Calabrese, C.; Poppleton, H.; Kocak, M.; Hogg, T. L.; Fuller, C.; Hamner, B.; Oh, E. Y.; Gaber, M. W.; Finklestein, D.; Allen, M.; Frank, A.; Bayazitov, I. T.; Zakharenko, S. S.; Gajjar, A.; Davidoff, A. & Gilbertson, R. J. (2007). A perivascular niche for brain tumor stem cells. *Cancer cell,* Vol.11, No.1, pp. 69-82, ISSN 1535-6108

Centonze, V. E. & White, J. G. (1998). Multiphoton excitation provides optical sections from deeper within scattering specimens than confocal imaging. *Biophysical Journal,* Vol.75, No.4, pp. 2015-2024, ISSN 0006-3495

Chaudhari, A. J.; Darvas, F.; Bading, J. R.; Moats, R. A.; Conti, P. S.; Smith, D. J.; Cherry, S. R. & Leahy, R. M. (2005). Hyperspectral and multispectral bioluminescence optical tomography for small animal imaging. *Physics in medicine and biology,* Vol.50, No.23, pp. 5421-41, ISSN 0031-9155

Choi, M.; Choi, K.; Ryu, S. W.; Lee, J. & Choi, C. (2011). Dynamic fluorescence imaging for multiparametric measurement of tumor vasculature. *Journal of Biomedical Optics,* Vol.16, No.4, pp. 046008, ISSN 1560-2281

Choi, M.; Ku, T.; Chong, K.; Yoon, J. & Choi C. (2011). Minimally Invasive Molecular Delivery into the Brain Using Optical Modulation of Vascular Permeability. *Proceedings of the National Academy of Sciences*, Vol.108, No.22, pp. 9256-61, ISSN 1091-6490

de Vries, N. A.; Bruggeman S. W.; Hulsman D.; de Vries H. I.; Zevenhoven J.; Buckle T.; Hamans B. C.; Leenders W. P.; Beijnen J. H.; van Lohuizen M.; Berns A. J. M. & van Tellingen O. (2010). Rapid and Robust Transgenic High-Grade Glioma Mouse Models for Therapy Intervention Studies. *Clinical Cancer Research,* Vol.16, No.13, pp. 3431-3441, ISSN 1078-0432

Denk, W.; Strickler J. H. & Webb W. W. (1990). Two-photon laser scanning fluorescence microscopy. *Science,* Vol.248, No.4951, pp. 73-6, ISSN 0036-8075

Drew, P. J.; Shih A. Y.; Driscoll J. D.; Knutsen P. M.; Blinder P.; Davalos D.; Akassoglou K.; Tsai P. S.& Kleinfeld D. (2010). Chronic optical access through a polished and reinforced thinned skull. *Nature methods,* Vol.7, No.12, pp. 981-4, ISSN 1548-7105

Farrar, C. T.; Kamoun W. S.; Ley C. D.; Kim Y. R.; Kwon S. J.; Dai G. P.; Rosen B. R.; di Tomaso E.; Jain R. K. & Sorensen A. G. (2010). In vivo validation of MRI vessel caliber index measurement methods with intravital optical microscopy in a U87 mouse brain tumor model. *Neuro-oncology,* Vol.12, No.4, pp. 341-350, ISSN 1522-8517

Finkelstein, S. D.; Black P.; Nowak T. P.; Hand C. M.; Christensen S. & Finch P. W. (1994). Histological characteristics and expression of acidic and basic fibroblast growth factor genes in intracerebral xenogeneic transplants of human glioma cells. *Neurosurgery,* Vol.34, No.1, pp. 136-43, ISSN 0148-396X

Fomchenko, E. I. & Holland E. C. (2006). Mouse models of brain tumors and their applications in preclinical trials. *Clinical Cancer Research,* Vol.12, No.18, pp. 5288-5297, ISSN 1078-0432

Gratton, E. (2011) Applied physics. Deeper tissue imaging with total detection. *Science,* Vol.331, No.6020, pp. 1016-7, ISSN 1095-9203

Hanahan, D.; Wagner E. F. & Palmiter R. D. (2007). The origins of oncomice: a history of the first transgenic mice genetically engineered to develop cancerle. *Genes & development,* Vol.21, No.18, pp. 2258-2270, ISSN 0890-9369

Hashizume, R.; Gupta N.; Berger M. S.; Banerjee A.; Prados M. D.; Ayers-Ringler J.; James C. D. & VandenBerg S. R. (2010). Morphologic and molecular characterization of ATRT xenografts adapted for orthotopic therapeutic testing. *Neuro-oncology,* Vol.12, No.4, pp. 366-76, ISSN 1523-5866

Hoffman, R. (2002). Green fluorescent protein imaging of tumour growth, metastasis, and angiogenesis in mouse models. *The lancet oncology,* Vol.3, No.9, pp. 546-56, ISSN 1470-2045

Hsu, A. R.; Hou L. C.; Veeravagu A.; Greve J. M.; Vogel H.; Tse V. & Chen X. (2006). In vivo near-infrared fluorescence imaging of integrin alphavbeta3 in an orthotopic glioblastoma model. *Molecular imaging and biology : MIB : the official publication of the Academy of Molecular Imaging,* Vol.8, No.6, pp. 315-23, ISSN 1536-1632

Huse, J. T. & Holland E. C. (2009). Genetically Engineered Mouse Models of Brain Cancer and the Promise of Preclinical Testing. *Brain Pathology,* Vol.19, No.1, pp. 132-143, ISSN 1015-6305

--- (2010). Targeting brain cancer: advances in the molecular pathology of malignant glioma and medulloblastoma. *Nature reviews. Cancer,* Vo.10, No.5, pp. 319-31, ISSN 1474-1768

Jensen, M. M.; Jorgensen J. T.; Binderup T. & Kjaer A. (2008). Tumor volume in subcutaneous mouse xenografts measured by microCT is more accurate and reproducible than determined by 18F-FDG-microPET or external caliper. *BMC medical imaging,* Vol.8, pp. 16, ISSN 1471-2342

Kalka, K.; Merk H. & Mukhtar H. (2000). Photodynamic therapy in dermatology. *Journal of the American Academy of Dermatology,* Vol.42, No.3, pp. 389-413; quiz 414-6, ISSN 0190-9622

Kienast, Y.; von Baumgarten L.; Fuhrmann M.; Klinkert W. E.; Goldbrunner R.; Herms J. & Winkler F. (2010). Real-time imaging reveals the single steps of brain metastasis formation. *Nature Medicine,* Vol.16, No.1, pp. 116-22, ISSN 1546-170X

Kircher, M. F.; Mahmood U.; King R. S.; Weissleder R. & Josephson L. (2003). A multimodal nanoparticle for preoperative magnetic resonance imaging and intraoperative optical brain tumor delineation. *Cancer research,* Vol.63, No.23, pp.8122-5, ISSN 0008-5472

Kovar, J. L.; Simpson M. A.; Schutz-Geschwender A. & Olive D. M. (2007). A systematic approach to the development of fluorescent contrast agents for optical imaging of mouse cancer models. *Analytical biochemistry,* Vol.367, No.1, pp. 1-12, ISSN 0003-2697

Kwon, C. H.; Zhao D.; Chen J.; Alcantara S.; Li Y.; Burns D. K.; Mason R. P.; Lee E. Y.; Wu H. & Parada L. F. (2008). Pten haploinsufficiency accelerates formation of high-grade astrocytomas. *Cancer research,* Vol.68, No.9, pp. 3286-94, ISSN 1538-7445

Levene, M. J.; Dombeck D. A.; Kasischke K. A.; Molloy R. P. & Webb W. W. (2004). In vivo multiphoton microscopy of deep brain tissue. *Journal of neurophysiology,* Vol.91, No.4, pp. 1908-12, ISSN 0022-3077

Manis, J. P. (2007). Knock out, knock in, knock down - Genetically manipulated mice and the Nobel Prize. *New England Journal of Medicine,* Vol.357, No.24, pp. 2426-2429, ISSN 0028-4793

Massoud, T. F. & Gambhir S. S. (2003). Molecular imaging in living subjects: seeing fundamental biological processes in a new light. *Genes & development,* Vol.17, No.5, pp. 545-80, ISSN 0890-9369

Morton, C. L. & Houghton P. J. (2007). Establishment of human tumor xenografts in immunodeficient mice. *Nature protocols,* Vol.2, No.2, pp. 247-50, ISSN 1750-2799

O'Neill, K.; Lyons S. K.; Gallagher W. M.; Curran K. M. & Byrne A. T. (2010). Bioluminescent imaging: a critical tool in pre-clinical oncology research. *The Journal of pathology,* Vol.220, No.3, pp. 317-27, ISSN 1096-9896

Orringer, D. A.; Chen T.; Huang D. L.; Armstead W. M.; Hoff B. A.; Koo Y. E. L.; Keep R. F.; Philbert M. A.; Kopelman R. & Sagher O. (2010). The Brain Tumor Window Model: A Combined Cranial Window and Implanted Glioma Model for Evaluating Intraoperative Contrast Agents. *Neurosurgery,* Vol.66, No.4, pp. 736-743, ISSN 0148-396X

Ozawa, T. & James C. D. (2010). Establishing Intracranial Brain Tumor Xenografts With Subsequent Analysis of Tumor Growth and Response to Therapy using Bioluminescence Imaging. *Journal of Visualized Experiments*. No.41, ISSN 1940-087X

Rehemtulla, A.; Stegman L. D.; Cardozo S. J.; Gupta S.; Hall D. E.; Contag C. H. & Ross B. D. (2000). Rapid and quantitative assessment of cancer treatment response using in vivo bioluminescence imaging. *Neoplasia,* Vol.2, No.6, pp. 491-495, ISSN 1522-8002

Shah, K. & Weissleder R. (2005). Molecular optical imaging: applications leading to the development of present day therapeutics. *NeuroRx : the journal of the American Society for Experimental NeuroTherapeutics,* Vol.2, No.2, pp. 215-25, ISSN 1545-5343

Slavine, N. V.; Lewis M. A.; Richer E. & Antich P. P. (2006). Iterative reconstruction method for light emitting sources based on the diffusion equation. *Medical physics,* Vol.33, No.1, pp. 61-8, ISSN 0094-2405

Stummer, W.; Pichlmeier U.; Meinel T.; Wiestler O. D.; Zanella F. & Reulen H. J. (2006). Fluorescence-guided surgery with 5-aminolevulinic acid for resection of malignant glioma: a randomised controlled multicentre phase III trial. *The lancet oncology,* Vol.7, No.5, pp. 392-401, ISSN 1470-2045

Sun, A.; Hou L.; Prugpichailers T.; Dunkel J.; Kalani M. A.; Chen X. Y.; Kalani M. Y. S. & Tse V. (2010). Firefly Luciferase-Based Dynamic Bioluminescence Imaging: A

Noninvasive Technique to Assess Tumor Angiogenesis. *Neurosurgery,* Vol.66, No.4, pp. 751-757, ISSN 0148-396X

Svaasand, L. O. & Ellingsen R. (1985). Optical Penetration in Human Intracranial Tumors. *Photochemistry and Photobiology,* Vol.41, No.1, pp. 73-76, ISSN 0031-8655

Szentirmai, O.; Baker C. H.; Bullain S. S.; Lin N.; Takahashi M.; Folkman J.; Mulligan R. C. & Carter B. S. (2008). Successful inhibition of intracranial human glioblastoma multiforme xenograft growth via systemic adenoviral delivery of soluble endostatin and soluble vascular endothelial growth factor receptor-2: laboratory investigation. *Journal of neurosurgery,* Vol.108, No.5, pp. 979-88, ISSN 0022-3085

Theer, P.; Hasan M. T. & Denk W. (2003). Two-photon imaging to a depth of 1000 microm in living brains by use of a Ti:Al2O3 regenerative amplifier. *Optics letters,* Vol.28, No.12, pp. 1022-4, ISSN 0146-9592

Torres Filho, I. P.; Hartley-Asp B. & Borgstrom P. (1995). Quantitative angiogenesis in a syngeneic tumor spheroid model. *Microvascular research,* Vol.49, No.2, pp. 212-26, ISSN 0026-2862

Tozer, G. M.; Ameer-Beg S. M.; Baker J.; Barber P. R.; Hill S. A.; Hodgkiss R. J.; Locke R.; Prise V. E.; Wilson I. & Vojnovic B. (2005). Intravital imaging of tumour vascular networks using multi-photon fluorescence microscopy. *Advanced Drug Delivery Reviews,* Vo.57, No.1, pp. 135-152, ISSN 0169-409X

Veiseh, M.; Gabikian P.; Bahrami S. B.; Veiseh O.; Zhang M.; Hackman R. C.; Ravanpay A. C.; Stroud M. R.; Kusuma Y.; Hansen S. J.; Kwok D.; Munoz N. M.; Sze R. W.; Grady W. M.; Greenberg N. M.; Ellenbogen R. G. & Olson J. M. (2007). Tumor paint: a chlorotoxin:Cy5.5 bioconjugate for intraoperative visualization of cancer foci. *Cancer research,* Vol.67, No.14, pp. 6882-8, ISSN 0008-5472

Weissleder, R. & Pittet M. J. (2008). Imaging in the era of molecular oncology. *Nature,* Vol.452, No.7187, pp. 580-9, ISSN 1476-4687

Wiesner, S. M.; Decker S. A.; Larson J. D.; Ericson K.; Forster C.; Gallardo J. L.; Long C.; Demorest Z. L.; Zamora E. A.; Low W. C.; SantaCruz K.; Largaespada D. A. & Ohlfest J. R. (2009). De novo Induction of Genetically Engineered Brain Tumors in Mice Using Plasmid DNA. *Cancer research,* Vol.69, No.2, pp. 431-439, ISSN 0008-5472

Wilson, B. C. & Patterson M. S. (1986). The physics of photodynamic therapy. *Physics in medicine and biology,* Vol.31, No.4, pp. 327-60, ISSN 0031-9155

Winkler, F.; Kienast Y.; Fuhrmann M.; Von Baumgarten L.; Burgold S.; Mitteregger G.; Kretzschmar H. & Herms J. (2009). Imaging glioma cell invasion in vivo reveals mechanisms of dissemination and peritumoral angiogenesis. *Glia,* Vol.57, No.12, pp. 1306-15, ISSN 1098-1136

Winkler, F.; Kozin S. V.; Tong R. T.; Chae S. S.; Booth M. F.; Garkavtsev I.; Xu L.; Hicklin D. J.; Fukumura D.; di Tomaso E.; Munn L. L. & Jain R. K. (2004). Kinetics of vascular normalization by VEGFR2 blockade governs brain tumor response to radiation: role of oxygenation, angiopoietin-1, and matrix metalloproteinases. *Cancer cell,* Vol.6, No.6, pp. 553-63, ISSN 1535-6108

Xu, H. T.; Pan F.; Yang G. & Gan W. B. (2007). Choice of cranial window type for in vivo imaging affects dendritic spine turnover in the cortex. *Nature Neuroscience,* Vol.10, No.5, pp. 549-551, ISSN 1097-6256

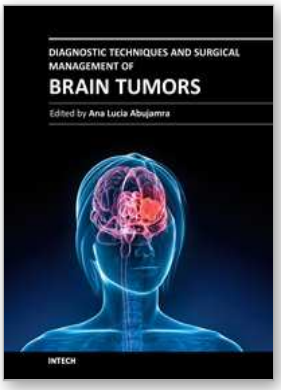

Diagnostic Techniques and Surgical Management of Brain Tumors
Edited by Dr. Ana Lucia Abujamra

ISBN 978-953-307-589-1
Hard cover, 544 pages
Publisher InTech
Published online 22, September, 2011
Published in print edition September, 2011

The focus of the book Diagnostic Techniques and Surgical Management of Brain Tumors is on describing the established and newly-arising techniques to diagnose central nervous system tumors, with a special focus on neuroimaging, followed by a discussion on the neurosurgical guidelines and techniques to manage and treat this disease. Each chapter in the Diagnostic Techniques and Surgical Management of Brain Tumors is authored by international experts with extensive experience in the areas covered.

How to reference
In order to correctly reference this scholarly work, feel free to copy and paste the following:

Kyuha Chong, Taeyun Ku, Kyungsun Choi, Myunghwan Choi, Jonghee Yoon and Chulhee Choi (2011). Current Optical Imaging Techniques for Brain Tumor Research: Application of in vivo Laser Scanning Microscopy Imaging with a Cranial Window System, Diagnostic Techniques and Surgical Management of Brain Tumors, Dr. Ana Lucia Abujamra (Ed.), ISBN: 978-953-307-589-1, InTech, Available from: http://www.intechopen.com/books/diagnostic-techniques-and-surgical-management-of-brain-tumors/current-optical-imaging-techniques-for-brain-tumor-research-application-of-in-vivo-laser-scanning-mi

INTECH
open science | open minds

InTech Europe
University Campus STeP Ri
Slavka Krautzeka 83/A
51000 Rijeka, Croatia
Phone: +385 (51) 770 447
Fax: +385 (51) 686 166
www.intechopen.com

InTech China
Unit 405, Office Block, Hotel Equatorial Shanghai
No.65, Yan An Road (West), Shanghai, 200040, China
中国上海市延安西路65号上海国际贵都大饭店办公楼405单元
Phone: +86-21-62489820
Fax: +86-21-62489821